Range and Capacity of LoRa 2.4 GHz

Reyhane Falanji, Martin Heusse, Andrzej Duda

Range and Capacity of LoRa 2.4 GHz

Reyhane Falanji, Martin Heusse, and Andrzej Duda

Univ. Grenoble Alpes, CNRS, Grenoble INP, LIG, F-38000 Grenoble, France
{first_name.last_name}@univ-grenoble-alpes.fr

Abstract. LoRa 2.4 GHz is a new variant of LoRa networks that uses the 2.4 GHz ISM band, different from the standard 868 MHz LoRa version. The LoRa physical layer takes advantage of a Chirp Spreading Spectrum (CSS) modulation with robust signals for transmission over long distances. While the standard LoRa in the 868 MHz band covers a range of 5-10 km, the actual capacity and range of LoRa 2.4 GHz are still not yet fully investigated. A shorter range is expected with the higher carrier frequency and an increased bandwidth. However, the wider bandwidth allows for the transmission of larger frames and a shorter airtime. In this study, we evaluate the coverage range and capacity of LoRa 2.4 GHz through precise simulations, taking into account a path loss model tailored for urban environments and frequencies over 2 GHz. We also take into account the effect of Rician or Rayleigh fading, as well as collisions in low and high load traffic conditions. The results show a maximum range of 1.1 km and capacity around 310 nodes for low traffic and the case in which each node in the network benefits from a minimum 60% Packet Delivery Ratio (PDR). This range drops to 700 m when the target PDR increases to 90%, accommodating 120 nodes. Under the assumption of Rayleigh fading and for the target PDR of 60 % and heavy load, the range attains 350 m with capacity of 30 nodes, and it drops to 120 m for the 90% target PDR.

Keywords: LoRa 2.4 GHz · LoRaWAN · Packet Delivery Ratio · Range · Capacity · Simulations

1 Introduction

In this paper, we consider the problem of evaluating the range and capacity of LoRa 2.4 GHz networks. This new variant specifies a physical layer based on Chirp Spread Spectrum (CSS) for IoT communications in the 2.4 GHz ISM band [1]. LoRa 2.4 GHz networks are similar to the standard LoRa defined in the sub GHz band: they use the same CSS modulation with the notion of the Spreading Factor (SF) and take advantage of the LoRaWAN MAC layer with the same frame structure and the unslotted ALOHA access method. The main difference with the standard LoRa is the use of a different frequency band with an increased data rate up to 254 kb/s for SF5, a larger 1625 KHz bandwidth, and the MAC payload size up to 248 B (SF5-SF10). The use of the 2.4 GHz band makes the coverage range smaller with the higher carrier frequency and

an increased bandwidth, which becomes of the order of 1 km compared to 5-10 km of the standard LoRa variant. However, the wider bandwidth allows for the transmission of frames of larger sizes and a shorter airtime.

The objective of this paper is to analyze the performance of LoRa 2.4 GHz networks in terms of the Packet Delivery Ratio (PDR), coverage, and capacity depending on different parameters such as SF, the environment type (channel characteristics), and the number of devices in a cell.

There are only a few studies of the LoRa 2.4 GHz performance [2,3,4,5,6,7,8]. They show that the coverage is smaller than the standard LoRa and the performance highly depends on the environment. Previous work analyzed the range and performance only depending on channel conditions (path loss and fading) and they did not take into account the influence of device contention and collisions. With an increasing number of devices, collisions are more likely to happen so they mostly limit the capacity of the network. Thus, in this study, we focus on both aspects: we use models to simulate collisions and take into account the channel propagation behavior with a path loss model tailored for urban environments and frequencies over 2 GHz as well as with Rician or Rayleigh fading to provide a more precise evaluation of the LoRa 2.4 GHz range and capacity.

In summary, we bring the following contributions:

- we develop and use a simulator written in Python to evaluate PDR in different cases,
- we present a set of results: i) first, to calibrate the simulation results, we compare them with reported measurements in an aquatic outdoor environment over a lake (the case of no collisions), ii) then, we valuate the performance of LoRa 2.4 GHz for the case of the SNR boundaries and maximal load due to the duty-cycle limitations of LoRa 868 MHz, and finally, iii) we perform extensive simulations for various levels of load, different target values of PDR, and fading models to evaluate the performance of LoRa 2.4 GHz.

The results show a maximum range of 1.1 km and capacity around 310 nodes for low traffic and the case in which each node in the network benefits from a minimum 60% Packet Delivery Ratio (PDR). This range drops to 700 m when the target PDR increases to 90%, accommodating 120 nodes. Under the assumption of Rayleigh fading and for the target PDR of 60 % and heavy load, the range attains 350 m with capacity of 30 nodes, and it drops to 120 m for the 90% target PDR.

Our study shows that LoRa 2.4 GHz can effectively support application traffic with higher intensity than the standard LoRa over a range of around 1 km depending on the target PDR and communication environments thus making LoRa 2.4 GHz a new kind of a “long-range Wi-Fi” network for supporting applications even beyond IoT.

The paper starts with a background on the LoRa 2.4 GHz characteristics (Section 2), we then discuss related work on LoRa modeling and measurements (Section 3), and describe the simulator (Section 4). Finally, we present a set of simulation results (Section 5).

Table 1: LoRa 868 MHz vs. 2.4 GHz

Transceiver	SX1278	SX1280
Frequency	868 MHz	2.4 GHz
Duty Cycle (EU)	1%	-
Max. Trans. Power	14 dBm	12.5 dBm
Max. Receiver Sensitivity	-148 dBm	-130 dBm (BW=203 kHz)
	-148 dBm	-120 dBm (BW=1625 kHz)

Table 2: Sensitivity and SNR limits.

SF	Sensitivity (dBm)	SNR_{limit}(dB)
5	-99	7
6	-103	3
7	-106	0
8	-109	-3
9	-111	-5
10	-114	-8
11	-117	-11
12	-120	-14

2 Background on LoRa 2.4 GHz

The standard LoRa devices operate in the sub-GHz ISM band (the 868 MHz band in Europe and the 915 MHz band in the US). The new LoRa variant takes advantage of the 2.4 ISM GHz band with a higher data rate and wider available bandwidth. The physical layer of LoRa has the following parameters [1]:

Bandwidth (BW) corresponds to the range of the frequency sweep done in CSS. It may have the following values: 203, 406, 812, and 1625 kHz within the band of 2.4 - 2.5 GHz.

Spreading Factor (SF) characterizes the number of bits carried by a chirp: SF bits are mapped to one of 2^{SF} possible frequency shifts in a chirp. SF varies between 5 and 12, with SF12 resulting in the best sensitivity and range, at the cost of the lowest data rate and worst energy consumption. Decreasing SF by 1 unit roughly doubles the transmission rate and divides by 2 the transmission duration as well as energy consumption.

Coding Rate (CR) – the rate of Forward Error Correction (FEC) that improves the packet error rate in presence of noise and interference. A lower coding rate results in better robustness, but increases the transmission time and energy consumption. The possible values are: 4/5, 4/6, 4/7, and 4/8.

Transmission Power (P) varies between -18 and 12.5 dBm.

Table 1 compares the main features of the two LoRa variants.

Receiver sensitivity (RS) determines to what extent the receiver can receive and demodulate the received signal, considering the existence of noise and collisions. RS depends on many factors, including the temperature, bandwidth, and

Table 3: Data rates for LoRa 2.4 GHz

BW (kHz)	Data rate DRj for SFj (kb/s)							
	SF5	SF6	SF7	SF8	SF9	SF10	SF11	SF12
203	32	19	11	6	4	2	1	0.6
406	63	38	22	13	7	4	2	1
812	127	76	44	25	14	8	4	2
1625	254	152	89	51	29	16	9	5

Table 4: LoRa 2.4 GHz parameters for 1625 kHz bandwidth [9]

SF	Max MAC payload (B)	Airtime (ms)
5	248	10.28
6	248	17.41
7	248	29.95
8	248	52.81
9	248	94.60
10	248	170.29
11	123	201.96
12	59	202.27

the noise figure (NF) and is given by:

$$\mathrm{RS} = -174 + 10\log_{10}\mathrm{BW} + \mathrm{NF} + \mathrm{SNR}_{\mathrm{limit}}. \tag{1}$$

Table 2 presents the values of RS for bandwidth of 1625 kHz and the Signal to Noise Ratio (SNR) limits for different spreading factors. Table 3 presents the available data rates for given bandwidth, for each SF. As expected, the data rate increases for larger bandwidth, but decreases as SF increases.

Regional duty cycle regulations restrict LoRa devices operating in sub-GHz frequency bands. The duty cycle depends on the frequency band: LoRa devices have to limit their occupation of each frequency band to 1% of time with 3 to 5 frequency channels in each band of 868 MHz in Europe. These duty cycle restrictions do not apply to the 2.4 GHz ISM band so devices may generate traffic with higher intensity. However, higher load may also lead to increased contention and worse performance when too many devices compete for the channel.

3 Related Work

3.1 Performance of the Standard LoRa

Many studies investigated the capacity of the standard LoRa networks either in a simulation setup [10,11,12], on real test beds [13,14,15,16], with mathematical/numerical analysis [17,18,19,20] or with hybrid methods [21,22,23]. They are not directly applicable to LoRa 2.4 GHz due to differences in their characteristics (i.e., duty cycle restrictions, SF ranges, etc.). Some simulations used models that might not be precise or proper for LoRa 2.4 GHz, for instance, path loss

propagation is mainly modeled as an exponential function, which does not reflect the realistic path loss behavior with sufficient accuracy.

3.2 Performance of LoRa 2.4 GHz

There are only a few studies of the LoRa 2.4 GHz performance.

Zhang et al. measured PDR in device-to-device communication experiments (no collisions) over a lake (mainly obstacle-free environment) achieving a 100% PDR over a range of 2.2 km (NLOS) to 2.7 km (LOS) for SF12 [2].

Polak et al. analyzed coexistence between Wi-Fi and LoRa 2.4 GHz to show high robustness of LoRa against interference [3]. Their results also reveal that LoRa robustness highly depends not only on the used LoRa system parameters, but also on the interferer properties and the assumed coexistence scenarios. To improve the coexistence of LoRa and Wi-Fi, Chen et al. proposed LoFi, a method for detecting weak signals [4].

Janssen et al. investigated the maximal theoretical communication range of LoRa 2.4 GHz in three different scenarios: free space, indoor, and urban path loss [5]. For the free-space channel model, a maximal theoretical range is 133 km while the same model results in the range of 921 km for the standard LoRa (roughly 7 times more). The authors estimated the maximal communication range in an urban environment of 443 m for SF12 and 203 KHz bandwidth.

Schappacher et al. have designed a LoRaWAN architecture that uses Time Slotted Channel Hopping (TSCH). They evaluate the communication range of LoRa 2.4 GHz with the designed architecture based on an indoor scenario. They measure the success rate by considering different frequencies, bandwidth, and SF. Measurements from this study show that the existence of walls can drastically reduce the delivery rate. However, with a lower bandwidth, a higher success rate can be achieved [6].

Wolf et al. explored the use of LoRa 2.4 GHz for two-way Time-of-Flight ranging with the Semtech SX1280 chip [7]. In this context, the authors concluded that two-way ranging exchanges fail for ranges greater than 500 m. In LOS conditions (straight road at the distance of 550 m), the ranging errors were inferior to 40 m in 50% of cases involving moving devices. Another study on the ranging capabilities of the SX1280 transceiver [8] reveals that the maximum reliable distance to measure with the chip is 1.7 km (with 100 requests per exchange). This study also shows that a higher SF is not necessarily a better setup and parameters such as bandwidth and SF should be set according to the distance.

Note that previous work analyzes the range and performance only depending on channel conditions (path loss and fading) and they do not take into account the influence of device contention and collisions. With an increasing number of devices, collisions are more likely to happen so they mostly limit the capacity of the network. Thus, in this study, we focus on both aspects: we use models to simulate collisions and take into account the channel propagation behavior to provide a more precise evaluation of the LoRa 2.4 GHz range and capacity.

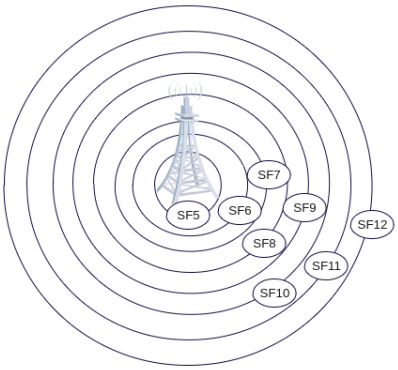

Fig. 1: Annuli of SF allocation around the gateway (the SF boundaries are equidistant in the figure, which is not the case in reality).

4 Simulator of LoRa 2.4 GHz

We have developed a discrete event simulator in Python for a single LoRa frequency channel used by a large number of nodes.[1] Compared to existing simulators such as NS-3, each experiment simulating a complete network with a large number of devices (e.g., hundreds of nodes) over 24 hours takes a few minutes only. In contrast, the same scenario would take considerably longer times with existing simulators. Moreover, the simulator implements an advanced collision model that detects signal decoding of interfering packets. To the best of our knowledge, no existing simulator of LoRa 2.4 GHz covers the requirements of our study.

In this simulator, we assume that devices are homogeneously scattered with spatial density ρ and they wake up to send data at intervals determined by applications, a usual assumption of IoT applications. Although devices may send packets at constant intervals, the sources are not synchronized, and they switch channel randomly so the superposition of traffic in a single channel coming from a large number of devices tends to a homogeneous Poisson process. We denote its intensity λ that depends on the data generation intensity of IoT applications and the number of frequency channels over which it is distributed.

For an increasing distance to the gateway, a device needs to change SF to maintain the desired level of PDR: further from the gateway, nodes need to use larger SF to increase the probability of frame reception. We can thus define SF boundaries around the gateway in form of concentric annuli in which devices share the same value of SF and the same frequency channel (see Figure 1) [21]. The number of nodes in a given SF zone is a function of the radii defining a given annulus around the gateway and the node density. The simulator assumes

[1] https://gricad-gitlab.univ-grenoble-alpes.fr/Drakkar-LIG/lora-2g4-simulator.git.

that all devices in a given SF zone use the same SFj (so each transmission has the same airtime and data rate DRj) and they contend for the same channel.

The simulator takes into account various channel propagation models, Rayleigh and Rician fading, the capture effect, as well as co-SF interference.

4.1 Channel Propagation Model

The simulator implements the ECC-33 model developed by Electronic Communication Committee [24]. It extends the earlier Okumura-Hata model [25,26] created based on the propagation experiment in Tokyo. However, it is only suitable for propagation of signals operating in frequencies from 150 to 1500 MHz. The ECC-33 model modified the assumptions of Okumura-Hata to adapt it for signals in 2 GHz bands, so corresponding to LoRa 2.4 GHz. The model defines the following path loss:

$$L_{ecc} = A_{fs} + A_{bm} - G_b - G_r, \tag{2}$$

where A_{fs}, A_{bm}, G_b, and G_r are the free space attenuation, the basic median path loss, base station height gain factor and receiver height gain factor, respectively, defined as follows:

$$A_{fs} = 92.4 + 20 \log d + 20 \log f, \tag{3}$$

$$A_{bm} = 20.41 + 9.83 \log d + 7.89 \log f + 9.56 (\log f)^2, \tag{4}$$

$$G_b = \log(\frac{h_b}{200})(13.958 + 5.8 log(d))^2, \tag{5}$$

$$G_r = (42.57 + 13.7 \log f)(\log h_r - 0.585), \tag{6}$$

where f is the frequency in GHz, d is the distance between the gateway and the LoRa transceiver in km, h_b is the gateway antenna height in meters, and h_r is the transceiver antenna height in meters.

Eq. 6 corresponds to a medium city environment. In case of large cities, the following equation for G_r applies:

$$G_r = 0.759 h_r - 1.862 \tag{7}$$

4.2 Fading Models

The simulator takes into account Rayleigh fading [16,21] that may greatly influence the packet reception for transmissions over long distances. The model assumes that a signal will randomly loose its strength or fade according to a

Rayleigh distribution—a multiplicative random variable with an exponential distribution of unit mean affects the received signal power.

We also consider Rician fading for comparisons with measurements. The simulation generates samples from a complex random variable $|X + jY|$, where X,Y are Gaussian random variables with non-zero mean and standard deviation that depend on a given K factor.

The Rayleigh and Rician fading model are used in combination with the ECC model.

4.3 Collision Model

The reference design of the LoRa 2.4 GHz gateway uses multiple transceivers—four SX1280 transceivers: three dedicated to reception and one to transmission allowing simultaneous reception over three LoRa modulated channels operating on a single, programmable spreading factor [27].

To consider collisions, the simulator uses a variation of the model of the standard LoRa [21] with two different types of collisions. When a device starts a transmission, the simulator analyzes other ongoing transmissions that may interfere. It computes the sum of the power of the existing interfering transmissions and, if it is more than the power of the present transmission minus a power capture margin of 6 dB, the simulator considers the new incoming frame as lost, as the receiver is unlikely to notice the newly arriving frame. Moreover, the simulator examines the effect of the present transmission on the other ongoing transmissions. If there is another ongoing transmission, the simulator adds the present transmission to the interference list of the other ongoing transmissions and eventually uses it to check if the sum of interfering powers is less than the frame power, for successful reception.

For the sake of simplicity, the simulator assumes that the interference from transmissions with other SFs is negligible as they are quasi-orthogonal [28,29]: except for rare near-far conditions, the gateway can receive simultaneous transmissions using different values of SF.

4.4 Simulation Setup

Table 5 summarizes the values of parameters for the simulation. We assume that packet arrival times are distributed according to a random exponential time (Poisson distribution of arrivals) with parameter λ. This assumption is justified if a large number of devices generate packets even if the intervals between packets are constant, a typical behavior of sensing devices. The simulator assumes the maximum possible value of 248 B for the size of the MAC payload (SF5 to SF10) to evaluate the cell capacity for the most stressing conditions (if not specified otherwise).

All presented simulation results have confidence intervals less than one percentage point so they are not marked on the graphs.

Table 5: Simulation parameters

Parameter	Value
Packet arrival intensity λ	1/12.33, 1/2 min^{-1}
Node density ρ	90, 900 nodes/km^2
Frequency	2.4 GHz
Bandwidth	406, 1625 kHz
Path loss model	ECC-33
Fading	Rician (K=100), Rayleigh
Simulation interval	24 hours
Gateway antenna height	17 m
Node antenna height	6 m
Transmission power	12.5 dBm

Table 6: Experimental results [2] vs. simulations for 406 kHz bandwidth and 16 B payload.

	Measured PDR	Range
Experimental	100%	2200 m
Simulation (no Rayleigh)	98%	2050 m
Simulation (Rician, K=100)	98%	1840 m
Simulation (Rayleigh)	98%	431 m

5 Simulation Results

In this section, we present the simulation results for different cases and scenarios.

5.1 Validation: Comparison with Reported Measurements

At the beginning, we compare the simulation results with the measurements done by Zhang et al. [2] in an outdoor environment over a lake. They measured PDR between two end-devices (no contention) over three distances: 1600 m, 2200 m, and 2700 m in different conditions of LOS, obstructed LOS, and NLOS. Even if the authors consider some cases as NLOS, devices are placed at the border of a lake, so that the environment rather corresponds to LOS or slightly obstructed LOS conditions. They used SX1280 modules with omnidirectional antennas (3 dBi) and the following parameters: transmission power of 12.5 dBm, bandwidth of 406 kHz, CR of 4/5, preamble length of 8 symbols, SF6 to SF12, and payload of 16 B.

An interesting case to compare with is the measurement over 2200 m that gives 100% PDR for SF12 and lower values of PDR for lower SFs, so it corresponds to a kind of a range limit. The LOS conditions were also satisfied for the case of 2700 m but we do not know if this distance is a range limit, because 100% PDR could have also be achieved for longer distances.

To compare with the measurements, we assume only one device per SF annulus in the simulation so there is no collision. Table 6 compares the simulation results with the measurements.

Table 7: SNR-based SF boundaries for the 1625 kHz bandwidth

PDR_{target}	SF5	SF6	SF7	SF8	SF9	SF10	SF11	SF12
70%	0.096	0.156	0.226	0.306	0.371	0.481	**0.636**	0.816

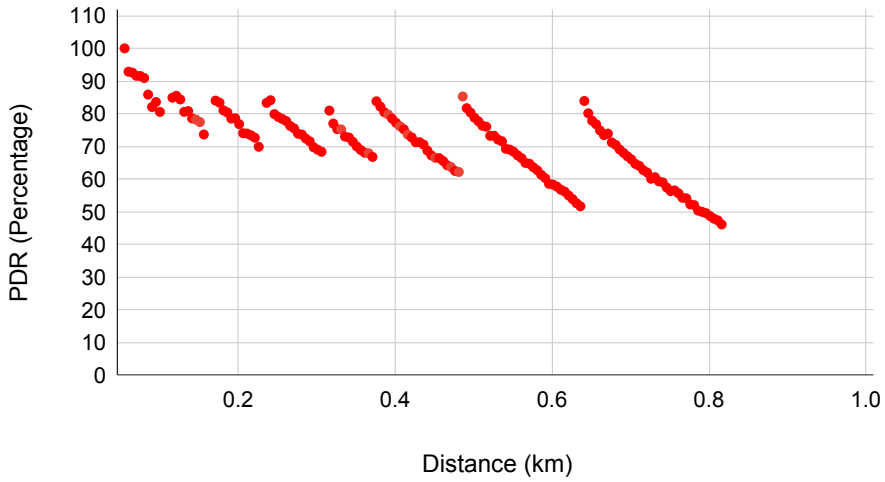

Fig. 2: Case of SNR boundaries and maximal load in the standard LoRa: cell radius of 0.636 km, node density ρ of 90 nodes per km^2, Rayleigh fading. Around 100 nodes in the distance of 0.590 km from gateway, using up to SF11 receive a PDR of at least 60%. Traffic intensity limited by the 1% duty cycle in the standard LoRa (1/12.33 min^{-1}).

The simulations give the results close to 2200 m when assuming the case of no Rayleigh and Rician path loss. Actually in the measurement experiments [2], although the scenario is presented as a NLOS case, the experimental environment corresponds to LOS conditions that are better represented with the Rician model. We can observe that taking into account Rayleigh fading results in a much shorter range.

In the rest of the evaluations, we use the Rician model representative of the measured environment and a model with Rayleigh fading that corresponds to a case of a dense urban environment.

5.2 Case of SNR Boundaries and Maximal Load in the Standard LoRa

In this section, we evaluate the performance of LoRa 2.4 GHz for the case of the SNR boundaries and maximal load analyzed for the standard LoRa [21] (Section 6.1). We use the most optimistic parameters of LoRa 2.4 GHz: bandwidth of 1625

kHz and the maximum payload of 248 B at the MAC layer. The simulations assume the same traffic load as used in the analysis of the standard LoRa cell capacity: all devices have the same interpacket generation interval that gives the 1% duty cycle for SF12 [21]: 1/12.33 min^{-1}. So, we address the following question: what would be the effect of upgrading standard LoRa devices to LoRa 2.4 GHz for the same application traffic?

For the standard LoRa [21], the SF boundaries were determined using an analytical model with a probability function of PDR—the SF boundary corresponds to the case for which the probability of successful packet delivery reaches a given target PDR (e.g., 60%). The *target PDR* corresponds to the minimum value that we want obtain in all annuli of a cell—we use two representative values: 90% or 60%. The target PDR of 90% may be sufficient enough for some data collecting applications. With 60% PDR, applications may obtain reliable data delivery by using some transmission redundancy in the form of inter-frame Error Correction Codes or transmission repetitions [13].

Computing SF boundaries is not possible if we use simulations, so we determine them by running the simulator first for a small number of nodes (no collisions) and we use the target PDR of 70% corresponding to PDR of 60% with a margin of 10% (see Table 7). Then, we run simulations with a given number of nodes determined by the node density of 90 nodes per km^2. For this density and the interpacket interval of 1/12.33 min^{-1}, collisions may happen so PDR may go down to 60%.

Figures 2 and 3 present the results for LoRa 2.4 GHz under the assumption of Rayleigh fading because this model was assumed for the analysis of the standard LoRa [21]. The fact of using the wider bandwidth of 1625 kHz in the 2.4 GHz band lowers the range compared to the standard LoRa—the boundary between SF11 and SF12 is at 636 m. Still, the capacity in terms of the number of devices is high: for the density of 90 nodes per km^2, the cell can have up to 100 nodes using up to SF11 benefiting from a PDR of at least 60% in the distance of 590 m (note that for longer distances, PDR goes below the target value of 60%). In the case of the standard LoRa, for the same node density, the boundary was at 3.59 km and 3648 nodes could benefit from PDR of at least 60% [21].

We have also evaluated the capacity of LoRa 2.4 GHz for a higher node density (900 nodes per km^2, not considered in the analysis of the standard LoRa) because the airtime is much shorter than in the standard LoRa. In this case, the number of collisions increases so the distance for getting PDR of at least 60% becomes smaller (280 m) but for a greater number of nodes (220).

5.3 Analysis of LoRa 2.4 GHz Capacity

In this section, we provide the results from running simulations of a LoRa 2.4 GHz network for various traffic intensities (1/2 and 1/12.33 min^{-1}) and for various node densities. For these results, we determine the SF boundaries between SF annuli for a given simulation setup in an iterative way to match the target PDR exactly.

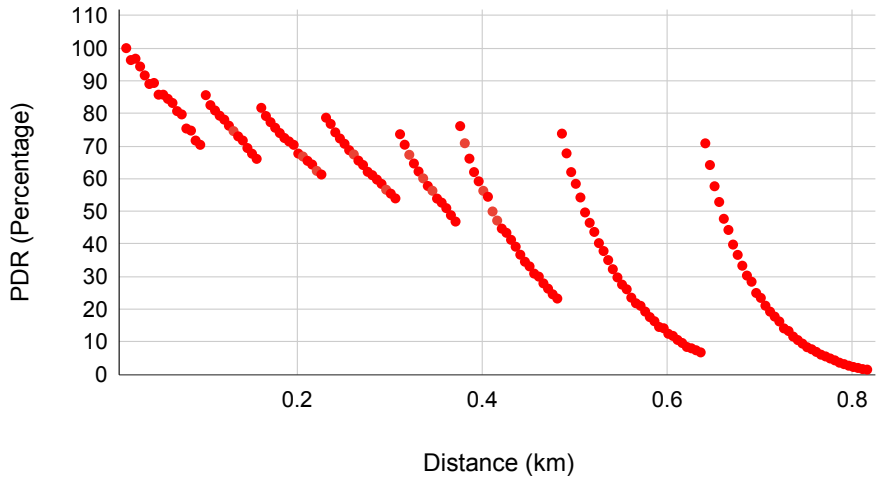

Fig. 3: Case of SNR boundaries and maximal load in the standard LoRa: cell radius of 0.636 km, node density ρ of 900 nodes per km^2, Rayleigh fading. Around 220 nodes in the distance of 0.280 km from gateway, using up to SF8 receive a PDR of at least 60%. Traffic intensity limited by the 1% duty cycle in the standard LoRa (1/12.33 min^{-1}).

Table 8: Capacity of a LoRa 2.4 GHz cell (number of nodes) for Rician fading

Target PDR	60%	90%
Low Load	310	120
High Load	210	40

The process starts with the initialization of the nodes in the first zone of SF5. Beginning with the zero distance from the gateway, we extend the border farther away with a fixed step size. Based on the selected node density ρ and the area of the zone delimited by the current border, we compute the number of nodes and place them at random distances within the area. The simulator generates packet transmissions at random instants and runs the discrete-event simulation to obtain the PDR of each node: it considers the transmission of the packet with the closest scheduled transmission time, keeps track of other possibly concurrent packet transmissions, and determines if there are collisions based on the timings and the power of transmissions. The number of successfully received packets gives us the PDR of each device in this zone.

If the minimum PDR of all nodes in the SF5 zone is still above the target PDR, we extend the border one step further and repeat the simulation to obtain the PDR of all nodes once again. When we reach the target PDR, the distance

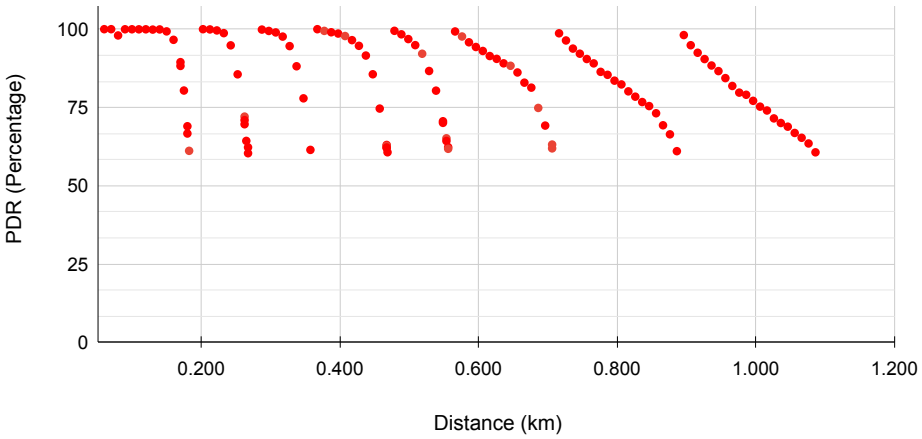

Fig. 4: Low load (density ρ of 90 nodes per km^2, traffic intensity of 1/12.33 min^{-1}), SF boundaries for target PDR of 60%, Rician fading. Cell capacity around 310 nodes.

Table 9: Capacity of a LoRa 2.4 GHz cell (number of nodes) for Rayleigh fading

Target PDR	60%	90%
Low Load	140	30
High Load	150	30

corresponds to the SF boundary. At this distance, the area of the next SF begins (SF6). We repeat this process for each SF up to SF12.

Figures 4 to 7 present PDR and capacity of a LoRa 2.4 GHz cell for different settings of load and target PDR under the assumption of Rician fading. We can observe that for low load (density ρ of 90 nodes per km^2, traffic intensity of 1/12.33 min^{-1}) and relaxed PDR condition of 60%, the cell range is fairly long with 1.1 km (see Figure 4). When we require the higher PDR of 90%, the range reduces to 700 m. Figures 6 to 7 present saturation conditions (high load—density ρ of 900 nodes per km^2, traffic intensity of 1/2 min^{-1}), with an increased impact of collisions and a much lower range (350 m, and 160 m, for 60% and 90% target PDR, respectively).

We also present similar cases but assuming Rayleigh fading (see Figures 8 to 11). For low load and target PDR of 60%, the cell range is shorter with 700 m (see Figure 8). For higher target PDR of 90%, the range reduces to 350 m (see Figure 9). Figures 10 to 11 correspond to saturation conditions so we can observe a larger number of collisions and a much lower range (250 m, and 120 m, for the 60% and 90% target PDR, respectively).

Tables 8 and 9 summarize the capacity in terms of the number of nodes for each case.

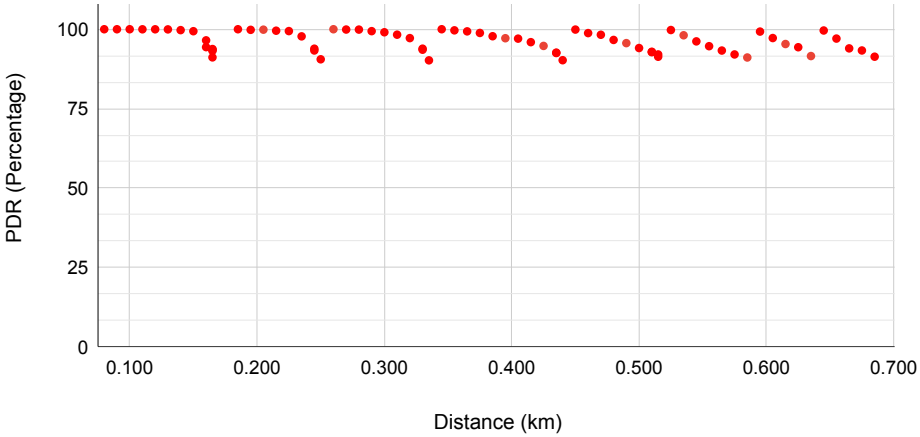

Fig. 5: Low load (density ρ of 90 nodes per km^2, traffic intensity of 1/12.33 min^{-1}), SF boundaries for target PDR of 90%, Rician fading. Cell capacity around 120 nodes.

6 Conclusion

In this paper, we have evaluated the capacity of a LoRaWAN network operating in the 2.4 GHz band. We have developed a discrete event simulator in Python that integrates a propagation model within an urban environment in GHz bands (ECC) with Rayleigh or Rician fading. It also models collisions and capture phenomena in a precise way.

To calibrate the simulation results, we have compared them with reported measurements for a specific case of an aquatic outdoor environment over a lake. Our simulator gives the results of the same order of magnitude.

We have then evaluated the performance of LoRa 2.4 GHz for the case of the SNR boundaries and the maximal application traffic determined by the 1% duty cycle of the standard LoRa. The range of the LoRa 2.4 GHz cell becomes much smaller—the boundary between SF11 and SF12 is at 636 m. The capacity in terms of the number of devices depends on the load: for low load, the cell can have up to 100 nodes using up to SF11 benefiting from a PDR of at least 60% in the distance of 590 m. For a higher node density, the number of collisions increases so the distance for getting PDR of at least 60% is smaller (280 m) but for a greater number of nodes (220).

Finally, we provide simulation results for LoRa 2.4 GHz in case of different traffic intensities (1/2 and 1/12.33 min^{-1}), various node densities (90 or 900 per km^2), the target PDR of 60% and 90%, and the fading model of Rician or Rayleigh. The results show that LoRa 2.4 GHz performance highly depends on channel load and the target PDR: the cell range can be fairly long (1.1 km) with capacity of 310 nodes benefiting from PDR of 60% for low load under the assumption of Rician fading. When load increases, the range becomes shorter (700 m) with lower capacity (210 nodes). Adopting the assumption of Rayleigh

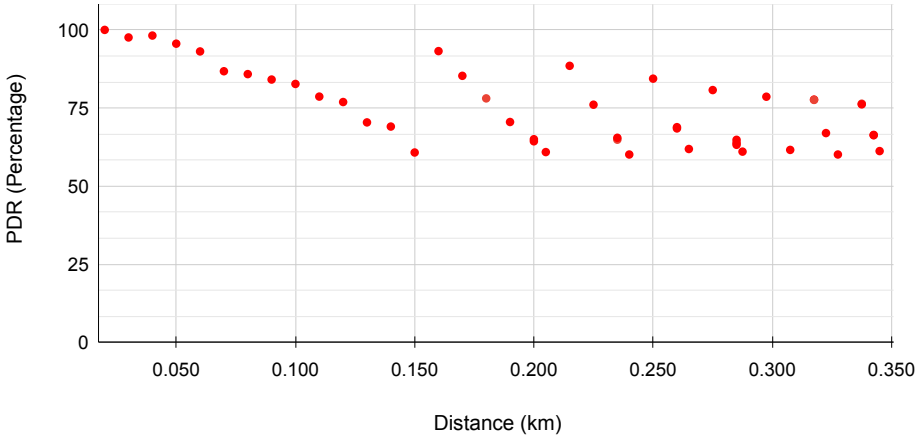

Fig. 6: High load (density ρ of 900 nodes per km^2, traffic intensity of 1/2 min^{-1}), SF boundaries for target PDR of 60%, Rician fading. Cell capacity around 210 nodes.

fading, which may correspond to a dense urban environment, results in a further decrease of the range and capacity.

In the future, we aim at experimental validation of the simulator to improve its capacity to emulate the realistic channel behavior in different environments.

Acknowledgments

This work has been partially supported by the French Ministry of Research projects PERSYVAL-Lab under contract ANR-11-LABX-0025-01 and DiNS under contract ANR-19-CE25-0009-01.

References

1. Semtech. SX1280/SX1281 Long Range, Low Power, 2.4 GHz Transceiver with Ranging Capability, DS.SX1280-1.W.APP, 2020.
2. Zheng Zhang, Shouqi Cao, and Yuntengyao Wang. "A Long-Range 2.4 GHz Network System and Scheduling Scheme for Aquatic Environmental Monitoring." Electronics 8.8 (2019): 909.
3. Ladislav Polak and Jiri Milos. "Performance Analysis of LoRa in the 2.4 GHz ISM Band: Coexistence Issues with Wi-Fi." Telecommunication Systems 74.3 (2020): 299-309.
4. Gonglong Chen, Wei Dong, and Jiamei Lv. "LoFi: Enabling 2.4 GHz LoRa and Wi-Fi Coexistence by Detecting Extremely Weak Signals." IEEE INFOCOM 2021-IEEE Conference on Computer Communications. IEEE, 2021.
5. Thomas Janssen et al. "LoRa 2.4 GHz Communication Link and Range." Sensors 20.16 (2020): 4366.

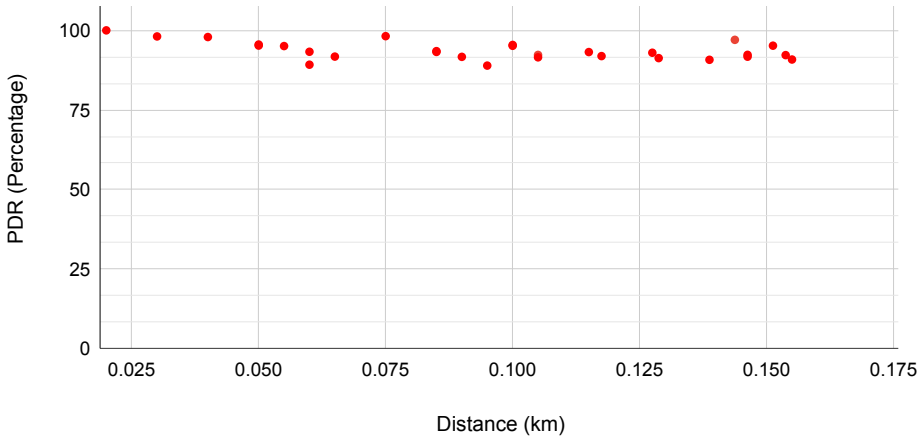

Fig. 7: High load (density ρ of 900 nodes per km^2, traffic intensity of 1/2 min^{-1}), SF boundaries for target PDR of 90%, Rician fading. Cell capacity around 40 nodes.

6. Manuel Schappacher, Amrut Dant, and Axel Sikora. "Implementation and Validation of LoRa-Based Systems in the 2.4 GHz Band." 2021 IEEE 4th International Conference on Advanced Information and Communication Technologies (AICT). IEEE, 2021.
7. Florian Wolf et al. "Benchmarking of Narrowband LPWA Physical Layer Ranging Technologies." 2019 16th Workshop on Positioning, Navigation, and Communications (WPNC). IEEE, 2019.
8. Frederik Andersen et al. "Ranging Capabilities of LoRa 2.4 GHz." 2020 IEEE 6th World Forum on Internet of Things (WF-IoT). IEEE, 2020.
9. https://lora-developers.semtech.com/documentation/tech-papers-and-guides\protect\discretionary{\char\hyphenchar\font}{}{}/physical-layer-proposal-2.4ghz, Semtech, 2021.
10. Floris Van den Abeele et al. "Scalability Analysis of Large-Scale LoRaWAN Networks in NS-3." IEEE Internet of Things Journal 4.6 (2017): 2186-2198.
11. Martin Bor et al. "Do LoRa Low-Power Wide-Area Networks Scale?" Proceedings of the 19th ACM International Conference on Modeling, Analysis and Simulation of Wireless and Mobile Systems. 2016.
12. Nadège Varsier and Jean Schwoerer. "Capacity Limits of LoRaWAN Technology for Smart Metering Applications." 2017 IEEE international Conference on Communications (ICC). IEEE, 2017.
13. Ulysse Coutaud, Martin Heusse, and Bernard Tourancheau. "High Reliability in LoRaWAN." 2020 IEEE 31st Annual International Symposium on Personal, Indoor and Mobile Radio Communications. IEEE, 2020.
14. Ulysse Coutaud, Martin Heusse, and Bernard Tourancheau. "LoRa Channel Characterization for Flexible and High Reliability Adaptive Data Rate in Multiple Gateways Networks." Computers 10.4 (2021): 44.
15. Rida El Chall, Samer Lahoud, and Melhem El Helou. "LoRaWAN Network: Radio Propagation Models and Performance Evaluation in Various Environments in Lebanon." IEEE Internet of Things Journal 6.2 (2019): 2366-2378.

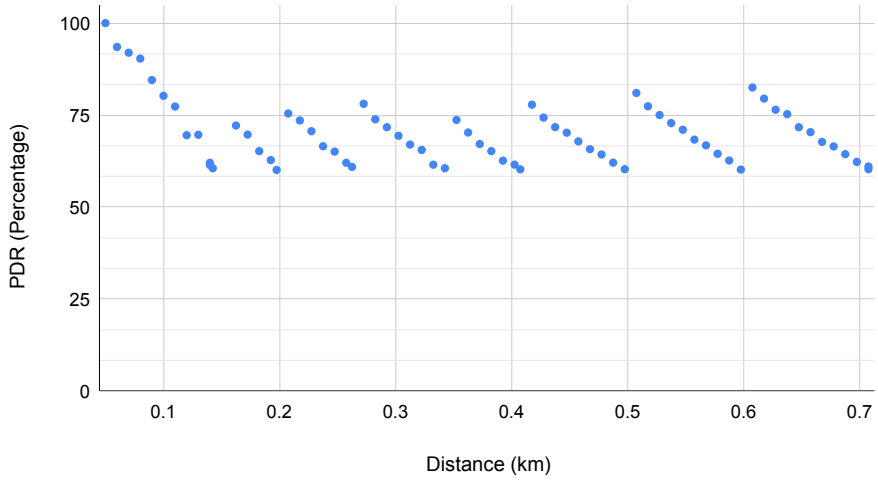

Fig. 8: Low load (density ρ of 90 nodes per km^2, traffic intensity of 1/12.33 min^{-1}), SF boundaries for target PDR of 60%, Rayleigh fading. Cell capacity around 140 nodes.

16. Takwa Attia et al. "Experimental Characterization of LoRaWAN Link Quality." 2019 IEEE Global Communications Conference (GLOBECOM). IEEE, 2019.
17. Orestis Georgiou and Usman Raza. "Low Power Wide Area Network Analysis: Can LoRa Scale?." IEEE Wireless Communications Letters 6.2 (2017): 162-165.
18. Konstantin Mikhaylov, Juha Petaejaejaervi, and Tuomo Haenninen. "Analysis of Capacity and Scalability of the LoRa Low Power Wide Area Network Technology." European Wireless 2016; 22th European Wireless Conference. VDE, 2016.
19. René Sørensen et al. "Analysis of Latency and MAC-Layer Performance for Class A LoRaWAN." IEEE Wireless Communications Letters 6.5 (2017): 566-569.
20. Andrzej Duda and Martin Heusse. "Spatial Issues in Modeling LoRaWAN Capacity." Proceedings of the 22nd International ACM Conference on Modeling, Analysis and Simulation of Wireless and Mobile Systems. 2019.
21. Martin Heusse, et al. "Capacity of a LoRaWAN Cell." Proceedings of the 23rd International ACM Conference on Modeling, Analysis and Simulation of Wireless and Mobile Systems. 2020.
22. Asif Yousuf et al. "Throughput, Coverage, and Scalability of LoRa LPWAN for the Internet of Things." 2018 IEEE/ACM 26th International Symposium on Quality of Service (IWQoS). IEEE, 2018.
23. Takwa Attia et al. "Message in Message for Improved LoRaWAN Capacity" 30th IEEE International Conference on Computer Communications and Networks, ICCCN 2021.
24. Electronic Communication Committee (ECC) within the European Conference of Postal and Telecommunications Administration (CEPT), "The Analysis of the Coexistence of FWA Cells in the 3.4 - 3.8 GHz Band", ECC Report 33, 2003
25. Yoshihisa Okumura. "Field Strength and its Variability in VHF and UHF Land-Mobile Radio Service." Rev. Electr. Commun. Lab. 16 (1968): 825-873.

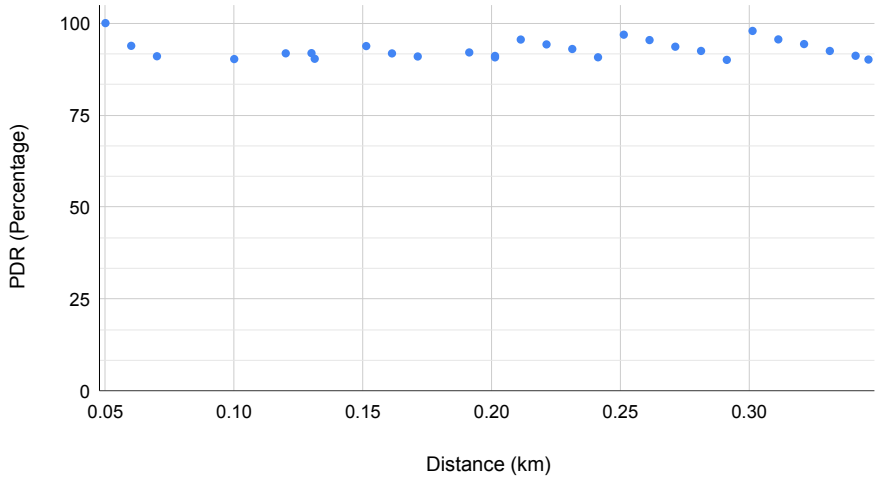

Fig. 9: Low load (density ρ of 90 nodes per km^2, traffic intensity of 1/12.33 min^{-1}), SF boundaries for target PDR of 90%, Rayleigh fading. Cell capacity around 30 nodes.

26. Masaharu Hata. "Empirical Formula for Propagation Loss in Land Mobile Radio Services." IEEE Transactions on Vehicular Technology 29.3 (1980): 317-325.
27. Semtech. LoRa 2.4 GHz 3 Channels Single SF Reference Design Performance Report, 2020.
28. Claire Goursaud and Jean-Marie Gorce. "Dedicated Networks for IoT: PHY/MAC State of the Art and Challenges." EAI Endorsed Transactions on Internet of Things (2015).
29. Aamir Mahmood et al. "Scalability Analysis of a LoRa Network under Imperfect Orthogonality." IEEE Transactions on Industrial Informatics 15.3 (2018): 1425-1436.

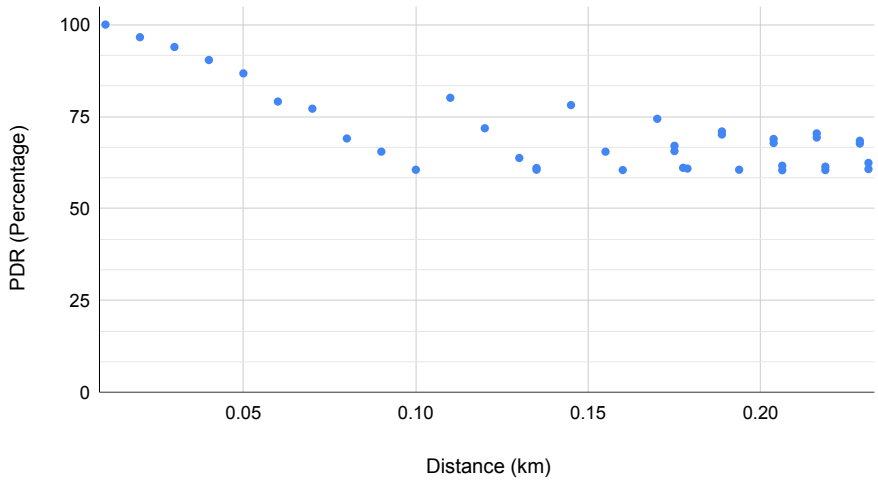

Fig. 10: High load (density ρ of 900 nodes per km^2, traffic intensity of 1/2 min^{-1}), SF boundaries for target PDR of 60%, Rayleigh fading. Cell capacity around 150 nodes.

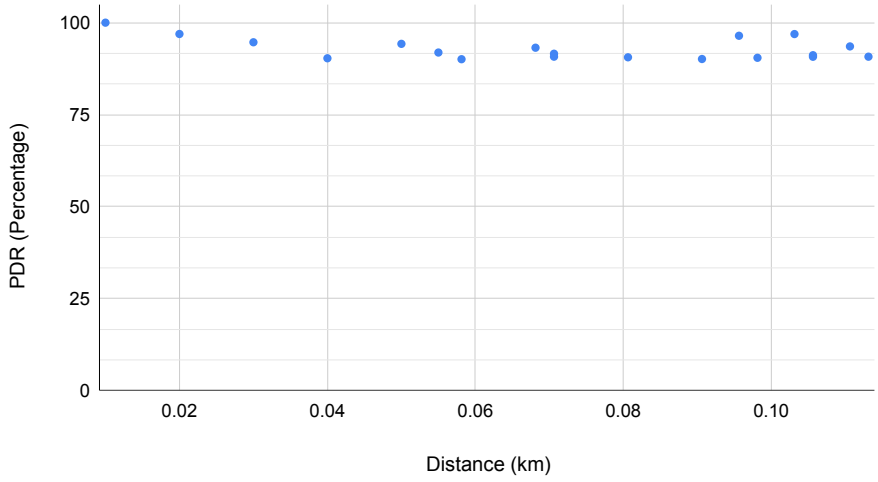

Fig. 11: High load (density ρ of 900 nodes per km^2, traffic intensity of 1/2 min^{-1}), SF boundaries for target PDR of 90%, Rayleigh fading. Cell capacity around 30 nodes.